Dalton Transactions

# Ionothermal synthesis, crystal structure, topology and catalytic property of heterometallic coordination polymers constructed from N-(phosphonomethyl) iminodiacetic acid



| | |
|---|---|
| Journal: | *Dalton Transactions* |
| Manuscript ID: | DT-ART-06-2015-002176.R1 |
| Article Type: | Paper |
| Date Submitted by the Author: | 21-Jun-2015 |
| Complete List of Authors: | Yang, Ting-Hai; Jiangsu University of Technology, School of Chemistry & Environmental Engineering; University of Aveiro, Department of Chemistry<br>Silva, Ana Rosa; University of Aveiro, Chemistry, CICECO; Unilever Discover Port Sunlight, Structured Materials Expertise Group<br>Fu, Lianshe; University of Aveiro,<br>SHI, Fa-Nian; University of Aveiro, Department of Chemistry, CICECO |
| | |

Dalton Transactions

RSCPublishing

ARTICLE

# Ionothermal synthesis, crystal structure, topology and catalytic property of heterometallic coordination polymers constructed from *N*-(phosphonomethyl) iminodiacetic acid

Cite this: DOI: 10.1039/x0xx00000x

Received 00th January 2015,
Accepted 00th January 2015

DOI: 10.1039/x0xx00000x

www.rsc.org/

Ting-Hai Yang,*[a,c] Ana Rosa Silva,[c] Lianshe Fu[d] and Fa-Nian Shi*[b,c]

Reactions of rare earth chlorides, *N*-(phosphonomethyl)iminodiacetic acid ($H_4$pmida) and ferrous oxalate dihydrate under ionothermal conditions result in four new isostructural 3*d*-4*f* heterometal coordination polymers, $[LnFe^{III}Fe^{II}_6(Hpmida)_6]\cdot 2H_2O$ {Ln = Eu (**1**), Dy (**2**), Ho (**3**) and Y (**4**)}. All compounds were characterized by infrared spectroscopy, elemental analysis, thermogravimetric analysis, X-ray diffraction. The compounds feature a very interesting three dimensional (3-D) structure built up from a secondary building unit, $[Fe_2(Hpmida)_2]^{2-}$ and possess a new topology type and complicated unique tilings. The catalytic properties of compounds **1**–**4** were investigated showing that this type of compound is a heterogeneous catalyst in the Knöevenagel condensation with high selectivity.

## Introduction

Ionothermal synthesis based on the use of ionic liquids (ILs) as solvents has gained increasing attention due to the outstanding properties of ILs: nonvolatility, wide reaction temperature range, high polarity, and so forth.[1-6] Recently, it has been explored and utilized in the fields of materials science and coordination polymers (CPs) because the reaction mechanisms between metal and organic components may differ from those of molecular environments under ionic environments.[7-10] Usually, ILs behave as solvents, structure-directing template, or charge-compensating groups in the reaction systems, thus the influence of both the cationic and anionic parts of ILs on the CPs structures have been studied.[11-15] Accordingly, it is feasible to synthesize CPs in ILs which have new structures and novel properties that are inaccessible from traditional methods.[16-20] We have reported several series CPs based on the ionothermal synthesis method.[21, 22]

The design and synthesis of transition metal–rare earth heterometallic coordination polymers (TMRECPs) are some of the most attractive areas of materials research.[23-26] The great interest in this area is driven by two major reasons: first, the introduction of a second metal centre may allow the construction of appealing novel topologies and beautiful architectures, and second, the incorporation of unusual metal coordination environments may influence the physical properties of the materials, especially their photoluminescent, magnetic and catalytic properties.[27-29] However, novel TMRECPs are difficult to obtain due to the fact that the competing coordination of transition metals (TM) and rare earth (RE) occurs to the same ligand. These complicated competing reactions very often lead to the generation of preferably homometallic complexes instead of heterometallic ones.

An effective strategy to obtain TMRECPs is the use of multiple coordination sites bifunctional or multifunctional ligands, such as amino acids,[30-32] iminodiacetic acid,[33-35] imidazoledicarboxylic acid[36-38] and pyridinecarboxylate,[39-41] that can hold TM and RE at the same time. While much attention has been focused on linkers with nitrogen-containing carboxylate, only limited reports have documented TMRECPs with phosphonate ligands.[21, 42-44]

At the same time, functionalized phosphonates such as nitrogen-containing phosphonates and carboxyphosphonates could be the best choice for the construction of TMRECPs because of their diverse coordinating sites and modes with different affinities towards different metal centres. Phosphonic acid, *N*-(phosphonomethyl) iminodiacetic acid ($H_4$pmida) with two additional carboxylic groups and one amine group, has been shown to be appropriate chelating ligand in a relatively acidic solution.

With the above considerations in mind, we explored heterometallic coordination polymers with three different functional groups that can potentially coordinate two metals through ionothermal synthesis method. Recently, we have reported that a series of novel TMRECPs based on pyrazole-3,5-dicarboxylic acid were an active and recyclable heterogeneous catalyst in the cyclopropanation of styrene.[29] Here we report the synthesis, structural analysis and catalysis of four TMRECPs with $H_4$pmida.

## Experimental

### Materials and methods

All the other starting materials were of reagent quality and were obtained from commercial sources without further purification. Elemental analyses for C, N and H were performed on a TruSpec 630-200-200 elemental analyser with a combustion furnace temperature of 1075 °C and an afterburner temperature of 850 °C. FT-IR spectra were collected from KBr pellets (Aldrich 99%+, FT-IR grade) on a Mattson 7000 FT-IR spectrometer in a range of 4000–400 $cm^{-1}$ at the resolution of 2 $cm^{-1}$. Thermogravimetric analyses (TGA) were carried out using a Shimadzu TGA 50 under air, from room temperature to ca. 700 ºC, with a heating rate of 10 ºC/min. Powder X-ray diffraction (PXRD) patterns were recorded at ambient temperature using an Empyrean diffractometer with Cu-Kα radiation ($\lambda$ = 1.54178 Å) in the 2$\theta$ range of 5 to 50° in reflection mode, which is equipped with a X'Celerator detector, a curved graphite-monochromated radiation and a flat-plate sample holder, in a Bragg-Brentano para-focusing optics configuration (45 kV, 40 mA).

In the catalytic experiments, the Knöevenagel condensation was performed at 60°C in batch reactors using 0.36 mmol benzaldehyde, 0.75 mmol malononitrile, 0.18 mmol of *n*-undecane (internal standard) and 0.1515 g of compound **1**, previously grinded, in 1.00 ml of toluene. To do the kinetic profiles of the reactions of compounds **1**–**4** they were performed using the same experimental conditions, but using 4.0 mL of toluene. The reaction was followed by GC, by withdrawing periodically aliquots from the reaction mixture, using a Bruker 450 GC gas chromatograph equipped with a fused silica Varian Chrompack capillary column VF-1 ms (15 m x 0.25 mm id; 0.25 µm film thickness) and using helium as carrier gas. The obtained products were confirmed using a Finnigan Trace GC-MS. After 27 hours of reaction the solution was decanted, filtered through 0.2 µm PTFE syringe filters to a new reactor and stirred at 60°C over the weekend. A control experiment was also performed using the same experimental procedure, but without addition of the CP **1**.

### Synthesis of compounds $[LnFe^{III}Fe^{II}_6(Hpmida)_6]\cdot 2H_2O$ {Ln = Eu (1), Dy (2), Ho (3) and Y (4)}

Compounds **1**–**4** were obtained under the same experimental conditions. In a general synthesis, a eutectic mixture (ionic liquid) was prepared by heating a mixture of choline chloride and malonic acid (CM) in a 1:1 mol ratio to 80 °C with constant magnetic stirring until a homogeneous transparent colourless liquid was formed.

To a mixture containing $H_4$pmida (3 mmol, 0.6813 g), $FeC_2O_4\cdot 2H_2O$ (3 mmol, 0.540 g) and $EuCl_3\cdot 6H_2O$ (0.5 mmol, 0.1805 g) [or $DyCl_3\cdot 6H_2O$ (0.1855 g) or $HoCl_3\cdot 6H_2O$ (0.1856 g) or $YCl_3\cdot 6H_2O$ (0.1517 g)] were added CM (8.0 g) and an aqueous solution of NaOH (0.5 M, 1.0 mL). The suspension was magnetically stirred for 1 h at ambient temperature in order to prepare a homogeneous sol, which was transferred to a Teflon-lined autoclave and placed inside a preheated oven at 150 °C for 72 h. After the autoclave is cooled to room temperature, gold block crystals of compound **1** suitable for single-crystal X-ray diffration analyses were isolated from final reaction products by filtration after washing several times with ethanol and distilled water, and dried in air at ambient temperature. The purities of the samples were confirmed by powder X-ray diffraction studies and elemental analyses. For **1**, Yield: 0.5214 g, 63%, based on $FeC_2O_4\cdot 2H_2O$. Anal. calcd for $C_{30}H_{46}O_{44}N_6P_6Fe_7Eu$: C, 18.73; H, 2.41; N, 4.40%. Found: C, 18.82; H, 2.48; N, 4.51%. IR (KBr, $cm^{-1}$): 3456(br), 2977(w), 2913(w), 1690(m), 1608(s), 1459(m), 1431(s), 1410(s), 1379(w), 1340(w), 1281(w), 1260(m), 1218(w), 1148(s), 1107(s), 1057(s), 993(m), 960(m), 927(m), 911(m), 868(m), 784(m), 718(w), 689(w), 630(w), 566(s), 529(m), 516(m), 458(w), 384(w), 311(w).

For **2**, Yield: 0.5132 g, 62%, based on $FeC_2O_4\cdot 2H_2O$. Anal. Found (calcd) for $C_{30}H_{46}O_{44}N_6P_6Fe_7Dy$: C, 18.63; H, 2.40%; N, 4.35. Found: C, 18.56; H, 2.36; N, 4.39%. IR (KBr, $cm^{-1}$): 3450(br), 2974(w), 2915(w), 1697(m), 1607(s), 1459(m), 1431(s), 1411(s), 1379(w), 1340(w), 1280(w), 1260(m), 1217(w), 1147(s), 1106(s), 1057(s), 993(m), 960(m), 927(m), 912(m), 868(m), 784(m), 718(w), 689(w), 630(w), 563(s), 529(m), 515(m), 458(w), 385(w), 310(w)..

For **3**, Yield: 0.4691 g, 56%, based on $FeC_2O_4\cdot 2H_2O$. Anal. Found (calcd) for $C_{30}H_{46}O_{44}N_6P_6Fe_7Ho$: C, 18.61; H, 2.39; N, 4.34%. Found: C, 18.76; H, 2.46; N, 4.39%. IR (KBr, $cm^{-1}$): 3460(br), 2975(w), 2915(w), 1696(m), 1606(s), 1459(m), 1432(s), 1412(s), 1379(w), 1340(w), 1281(w), 1261(m), 1218(w), 1147(s), 1108(s), 1057(s), 994(m), 962(m), 927(m), 912(m), 870(m), 784(m), 720(w), 690(w), 630(w), 564(s), 531(m), 513(m), 459(w), 388(w), 309(w).

For **4**, Yield: 0.3441 g, 42%, based on $FeC_2O_4\cdot 2H_2O$. Anal. Found (calcd) for $C_{30}H_{46}O_{44}N_6P_6Fe_7Y$: C, 19.36; H, 2.49; N, 4.52. Found: C, 19.46; H, 2.56; N, 4.59 %. IR (KBr, $cm^{-1}$): 3450(br), 2975(w), 2914(w), 1697(m), 1607(s), 1462(m), 1431(s), 1411(s), 1379(w), 1340(w), 1278(w), 1261(m), 1217(w), 1149(s), 1105(s), 1057(s), 993(m), 959(m), 927(m), 913(m), 866(m), 786(m), 719(w), 688(w), 630(w), 563(s), 530(m), 515(m), 458(w), 385(w), 309(w).

### X-ray crystallographic analysis

Single crystals with dimensions 0.08×0.06×0.04 mm for **1**, 0.16×0.16×0.14 mm for **2,** 0.10×0.10×0.08 mm for **3**, and 0.16×0.12×0.12 mm for **4** were selected for indexing and intensity date collection at 298 K on a Bruker SMART APEX-II CCD diffractometer equipped with graphite-monochromatized Mo *Kα* ($\lambda$ = 0.71073Å) radiation. A hemisphere of date was collected in the $\theta$ range 3.77-28.29° for **1**, 1.78-25.99° for **2**, 2.36-25.99° for **3**, and 2.36-25.99° for **4** using a narrow-frame method with scan widths of 0.30° in $\omega$ and an exposure time of 10s per frame. Numbers of measured and observed reflections [$I>2\sigma(I)$] are 9435 and 2577 ($R_{int}$ = 0.0715) for **1**, 7855, 2019 ($R_{int}$= 0.0527) for **2**, and 8237 and 2021 ($R_{int}$= 0.0393) for **3**, and 8116 and 2016 ($R_{int}$= 0.0550) for **4** respectively. The date was integrated using the Siemens SAINT program,[45] with the intensities corrected for Lorentz factor, polarization, air absorption, and absorption due to variation in the path length through the detector faceplate.

The structures were solved by direct method using SHELXS-97[46] and refined on $F^2$ by full matrix least-squares using SHELXL-97.[47] All the non-hydrogen atoms were refined anisotropically. All H atoms were refined isotropically. Crystallographic and refinement details are listed in Table 1. Selected bond lengths and angles are given in Tables S1 and Table S2. CCDC reference numbers: 1055583–1055586 correspond to compounds **1**–**4**, respectively.

 

**Table 1** Crystallographic data for compounds **1**–**4**

| Compound | **1 (Eu)** | **2 (Dy)** | **3 (Ho)** | **4 (Y)** |
|---|---|---|---|---|
| Empirical formula | $C_{30}H_{46}O_{44}N_6P_6Fe_7Eu$ | $C_{30}H_{46}O_{44}N_6P_6Fe_7Dy$ | $C_{30}H_{46}O_{44}N_6P_6Fe_7Ho$ | $C_{30}H_{46}O_{44}N_6P_6Fe_7Y$ |
| F. w. | 1923.46 | 1934.00 | 1936.43 | 1912.41 |
| Crystal system | Trigonal | Trigonal | Trigonal | Trigonal |
| Space group | R-3 | R-3 | R-3 | R-3 |
| $a = b$ ( Å) | 15.3720(4) | 15.2875(5) | 15.2935(4) | 15.3080(3) |
| $c$ (Å) | 22.8499(2) | 22.7526(2) | 22.7749(1) | 22.7261(1) |
| $\alpha = \beta$ (°) | 90 | 90 | 90 | 90 |
| $\gamma$ (°) | 120 | 120 | 120 | 120 |
| $V$( Å$^3$) | 4676.0(4) | 4661.6(2) | 4613.2(2) | 4612.0(2) |
| Z | 3 | 3 | 3 | 3 |
| $D_c$ (g/cm$^3$) | 2.049 | 2.092 | 2.091 | 2.009 |
| $\mu$ (mm$^{-1}$) | 2.836 | 3.076 | 3.142 | 2.804 |
| $F$(000) | 2865 | 2874 | 2877 | 2793 |
| GOF on $F^2$ | 1.029 | 1.064 | 1.047 | 1.008 |
| $R_1$, $wR_2$ [a] | 0.0566, | 0.0487, | 0.0470, | 0.0448, |
| [$I$>2σ($I$)] | 0.1079 | 0.1491 | 0.1361 | 0.1380 |
| $R_1$, $wR_2$ [a] | 0.0962, | 0.0600, | 0.0554, | 0.0682, |
| (All date) | 0.1222 | 0.1551 | 0.1398 | 0.1465 |
| (Δρ)max, | 1.189, | 1.711, | 2.481, | 1.052, |
| (Δρ)min | -1.001 | -1.204 | -1.425 | -0.825 |
| (eÅ$^{-3}$) | | | | |

[a] $R_1 = \Sigma||F_o| - |F_c||/\Sigma|F_o|$, $wR_2 = [\Sigma w(F_o^2 - F_c^2)^2/\Sigma w(F_o^2)^2]^{1/2}$

## Results and discussion

### Description of Structures

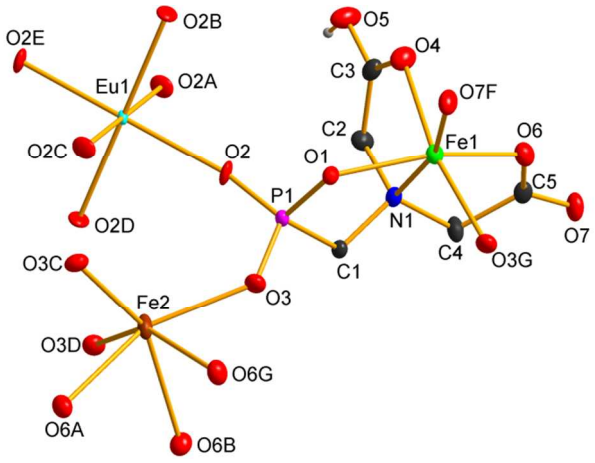


Fig. 1 Building unit of **1** with the atomic labeling scheme (30% probability). All H atoms except that attached to O5 were omitted for clarity. Symmetry codes are the same as those given in Table S1.

Compounds **1**–**4** are isostructural, and crystallizes in trigonal lattice with *R-3* space group. hence only the structure of **1** will be discussed in detail as representative. The asymmetric unit of **1** consists of one $Fe^{2+}$ ion, one-sixth $Fe^{3+}$ ion, one-sixth $Eu^{3+}$ ion, one $Hpmida^{3-}$ ligand and one-third lattice water molecule. As shown in Fig.1, the three metal ions ($Eu^{3+}$, $Fe^{3+}$, and $Fe^{2+}$) are all six-coordinated with a distorted octahedral geometry. Around the $Eu^{3+}$(1) ion, six positions are occupied by six phosphonate oxygen atoms [O(2), O(2A), O(2B), O(2C), O(2D), O(2E)] from six equivalent $Hpmida^{3-}$ ligand. The $Fe^{2+}$(1) ion is surrounded by two phosphonate oxygen[O(1), O(3G) ] from two equivalent $Hpmida^{3-}$ ligand, three carboxylate oxygen atoms [O(4), O(6), O(7F)] from two equivalent $Hpmida^{3-}$ ligand and one nitrogen atom [N(1)]. The $Fe^{3+}$(2) ion has a highly distorted octahedral environment with Fe(2) being bonded by three phosphonate oxygen[O(3), O(3C), O(3D) ] from three equivalent $Hpmida^{3-}$ ligand and three carboxylate oxygen atoms [O(6A), O(6B), O(6G)] from three equivalent $Hpmida^{3-}$ ligand. The Fe–O(N) bond lengths range from 2.102(5) to 2.479(5) Å with slightly longer Fe(2)-O6 bond [2.479(5) Å] and the Eu–O bond lengths are all 2.292(4) Å (Table 2). which are comparable to those 3*d*–4*f* heterometal coordination polymers.[48, 49]

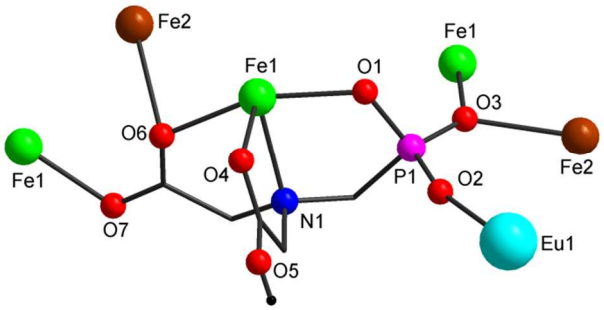


Fig.2 coordination mode of $Hpmida^{3-}$ ligand.

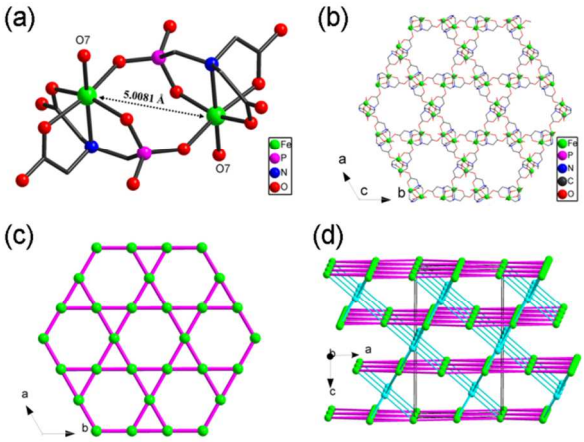


Fig. 3 (a) The dimeric unit structre $[Fe_2(Hpmida)_2]^{2-}$ in compound **1**; (b) Layer structure construted from $[Fe_2(Hpmida)_2]^{2-}$ unit in **1**; (c) Layer topological structure of **1**. green ball, $[Fe_2(Hpmida)_2]^{2-}$ unit; (d) The topological structure of connections between layers in **1**. cyan ball, Eu atom; green ball, $[Fe_2(Hpmida)_2]^{2-}$ unit.

The carboxylate oxygen atom O(5) of the $Hpmida^{3-}$ ligand is protonated. The $Hpmida^{3-}$ anion serves as a nine-dentate ligand,

chelating one $Fe^{2+}$ ion, bridging two $Fe^{2+}$ ions, two $Fe^{3+}$ ions and one $Eu^{3+}$ ion, respectively, in a $\mu_9$-$\eta^4$N,O,O,O, $\eta^1$O, $\eta^1$O', $\eta^1$O'', $\eta^1$O''' fashion (Fig. 2). Thus, the ligand traps effectively the $Fe^{2+}$ center [Fe(1)] inside three five-membered chelating rings. Two such chelates are linked to form the dimeric unit $[Fe_2(Hpmida)_2]^{2-}$(Fig.3a), in which the distances between the symmetric Fe(1) is 5.0081(13) Å. The dimer and symmetric dimer are alternatively bridged by the carboxylate oxygen (O7) of $Hpmida^{3-}$ to form an infinite layer in the *ab* plane (Fig. 3b). If the dimer was taken as a node, each dimeric unit is connected to another four dimers, forming a Kagome structure plane net whose tiling is composed of triangles and hexagons (Fig. 3c).

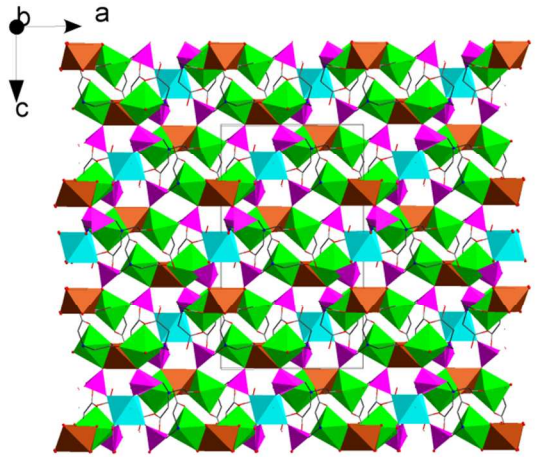


Fig. 4 The packing structure of **1** viewed along the b-axis. All H atoms are omitted for clarity. Cyan polyhedron, coordinated Eu ion; green polyhedron, coordinated $Fe^{2+}$ ion; brown polyhedron, coordinated $Fe^{3+}$ ion; pink polyhedron, $CPO_3$ group.

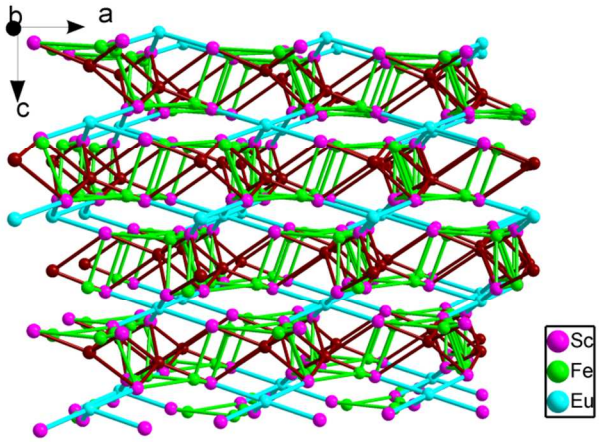


Fig. 5 The topology structure of **1**. pink ball, ligand; cyan ball, $Eu^{3+}$; green ball, $Fe^{2+}$; brown ball, $Fe^{3+}$.

Remarkably, connections between these adjacent layers formed by the anionic $[Fe_2(Hpmida)_2]^{2-}$ dimeric units are reinforced by the octahedral Eu atom (Fig. 3d), which connect to the external phosphonate oxygen (O2) (Fig. S1). Consequently, a 3-D heterometallic framework (Fig. 4), thus, is constructed by linking these 2-D layers via six coordinated Eu atoms. The overall framework is characterized by the presence of large empty voids which can contain lattice water molecules and charge-balancing coordinated $Fe^{3+}$ cations.

To further understand the topological structure of these metal phosphonates, we examined the connection mode of the metal centers and organic ligands. All topological studies were performed with the software package TOPOS[50] and only the covalent bonds in the structure were considered. In the compound **1**, each crystallographically independent metal center is taken as a node, with intermetal bridges ensured by the bridging ligand. Due to its crucial structural importance, i.e., connectivity to more than two metallic centers ($\mu_n$), the center of gravity of the ligand ($Hpmida^{3-}$) was also considered as a network node. Each $Eu^{3+}$ ions is connected to six $Hpmida^{3-}$ ligands, and is viewed as a 6-connected node. Each $Fe^{3+}$ and $Fe^{2+}$ ions, in turn, are connected to six and three $Hpmida^{3-}$ ligands, and is considered a 6-connected node and 3-connected node, respectively. The $Hpmida^{3-}$ ligand connects one $Eu^{3+}$, two $Fe^{3+}$ and three $Fe^{2+}$ ions and is viewed as a 6-connected node. The final network is, thus, tetranodal, 3,6,6,6-connected, with an overall point symbol of $\{4^{12}\cdot6^3\}_2\{4^3\}_6\{4^6\cdot8^6\cdot10^3\}\{4^8\cdot6^6\cdot8\}_6$ (Fig. 5). The latest TTD database indicates that this nodal connectivity is unprecedented among CP structures, thus we deposit it as fnc3 in the TTD database.

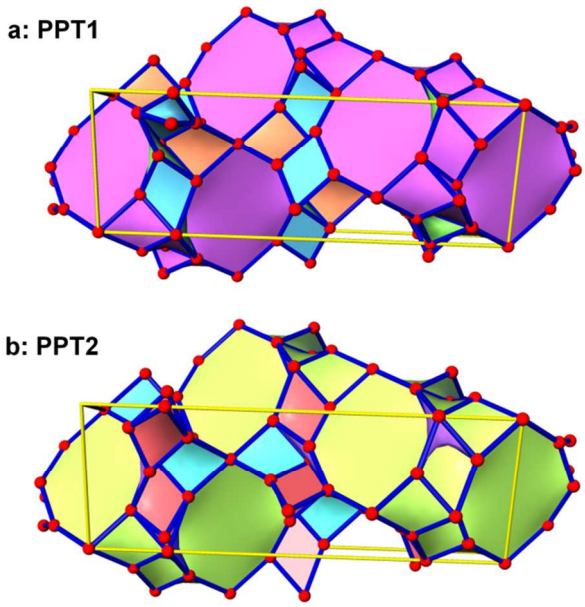


Fig. 6 two typical tiling nets of compound **1** along *x* axis showing very similar features and having the same transitivity of [4674].

Using 3DT and Topos 4 programs[50] to study on the tilings of net **1** shows that there are two primitive proper tilings (PPT1 and PPT2 Fig. 6) in the unit cell and natural tiling cannot be constructed. There are four kinds of tiles in PPT1 and PPT2 (Fig. 6) corresponding to $2[4^3]$, $6[4^3]$, $6[4^3]$ and $[4^{24}.8^6]$ (represented in four different colours). TOPOS analysis also revealed the presence of 7 essential rings (4a, 4b, 4c, 4d, 4f, 4g, 8b for PPT1 and 4a, 4b, 4d, 4e, 4f, 4g, 8b for PPT2) for each tiling in this 3-D net, which indicate the PPT1 and

PPT2 are quite similar with the same transitivity of [4674]. These 7 essential rings contain six 4-membered rings and one 8-membered ring that are organized together to build this complicated architecture.

The structures of compounds **2**–**4** are analogous to **1** except that the $Eu^{3+}$ ion in **1** is replaced by $Dy^{3+}$ in **2**, $Ho^{3+}$ in **3** and $Y^{3+}$ in **4**. The cell volumes decrease in turn from **1** to **4**, in accordance with the decreasing sequence of the ionic radii of the corresponding metal ions due to the lanthanide contraction.

### IR Spectra

The IR spectra for compounds **1**−**4** were recorded in the region from 4000−400 $cm^{-1}$ (Figures S2−S4). The presence of lattice and coordination water molecules is manifested by a broad IR band of medium intensity in the range of about 3500 $cm^{-1}$, assigned to ν(OH). The C−H stretching vibrations are observed as sharp, weak bands close to 2900 $cm^{-1}$. The absorption bands at 1697 $cm^{-1}$ are assigned to the vibration of protonated carboxylate group, which agrees with the single X-ray crystal structure analyses. The strong peaks at 1700–1300 $cm^{-1}$ are assigned to the asymmetric and symmetric vibrations of the coordinated carboxylate groups. The set of bands between 1200 and 900 $cm^{-1}$ are assigned to stretching vibrations of the tetrahedral $CPO_3$ groups. Additional weak bands at low energy for these compounds are found. These bands are probably due to bending vibrations of the tetrahedral $CPO_3$ groups.

### PXRD and thermal stability

The experimental and simulated powder X-ray diffraction (PXRD) patterns of complexes **1**–**4** are shown in Fig. 7. The experimental PXRD patterns at room temperature are in good agreement with the simulated one based single-crystal X-ray solution, indicating the phase purity of the bulk products. The differences in reflection intensities are probably due to the preferred orientation effects.

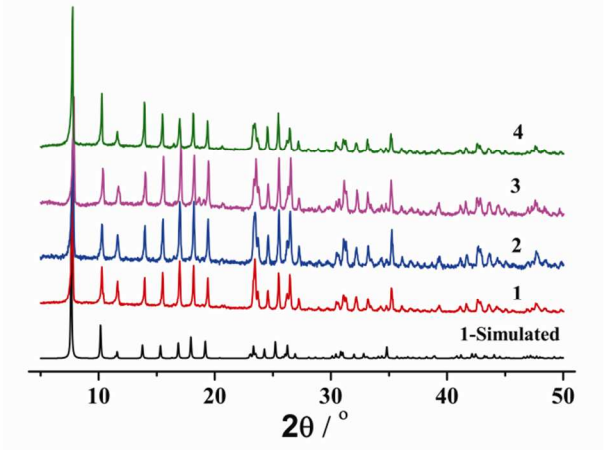


Fig. 7 Experimental and simulated PXRD patterns of **1**–**4**.

Thermal analyses were carried out for **1**–**4** to examine the thermal stabilities of these complexes (Fig. S5). The thermogravimetry curves of **1**–**4** display similar thermal behaviours and good thermal stability (up to 250 °C) in air, presumably due to the framework stabilization of the 3-D network. The weight losses observed up to 250 °C are attributed to the gradual release of the confined water molecules from the structure cavities. The weight loss above 250 °C is due to the decomposition of the compounds and the collapse of the lattice. The final residue was not characterized.

### Catalytic property

Some CPs have been studied as heterogeneous catalysts in the Knöevenagel condensation (Fig. 8).[51] This is an important C−C coupling reaction of a carbonyl group with a compound containing an activated methylene group (Fig. 8) and is widely used for the synthesis of fine chemicals and pharmaceuticles.[52] Thus compound **1** was tested as heterogeneous catalyst in the Knöevenagel condensation of benzaldehyde with malononitrile in 1.0 mL toluene at 60°C. The material showed catalytic activity in this reaction when compared to the control experiment performed using exactly the same experimental conditions, but without the addition of the catalyst. After 27 hours of reaction the benzaldehyde conversion was 27%, whereas for the control experiment 7% was obtained. The turnover number (TON) was 119 for the reaction with compound **1** and the corresponding turnover frequency (TOF) was 4.4 $h^{-1}$. In both reactions the major product observed was the expected Knöevenagel condensation product (Fig. 8)[51] with 98 and 95% selectivity, respectively. Benzoic acid was observed as minor product. After the 27 hours of reaction, the solution was separated from the heterogeneous catalyst by decantation and it was filtered, using syringe filters, to a new reactor. After a weekend stirring (68 hours) at 60 °C no further significant catalytic activity was observed (%C=29), proving that the observed 27% benzaldehyde conversion was from the compound **1** and that the reaction was truly heterogeneous. After convenient washing with toluene, the filtered material was used in a second catalytic cycle, using the same experimental conditions. After 27 hours a benzaldehyde conversion of 32% was obtained with a TON of 165 and TOF of 6.1 $h^{-1}$. In a third catalytic cycle of reuse and after the 27 hours the benzaldehyde conversion was 28%, TON of 161 and TOF of 6.0 $h^{-1}$. In a fourth catalytic cycle of reuse and after the 27 hours the benzaldehyde conversion was 8%, TON of 86 and TOF of 3.2 $h^{-1}$. After the second cycle, the PXRD pattern of **1** is similar to the as-synthesized (Fig. S7). Thus the material could be recycled and reused at least for two more catalytic cycles without loss of catalytic activity. The substrate scope was also extended to *o*-tolualdehyde and heptaldehyde. The reaction with malononitrile of *o*-tolualdehyde gave an aldehyde conversion of 20% in 4.0 mL of toluene at 60°C, with TON of 94 and TOF of 3.2 $h^{-1}$ (27 hours of reaction). No by-products were detected indicating that the reaction was selective for the Knöevenagel condensation product. And the reaction of malononitrile with heptaldehyde in 1.0 mL of toluene at 60°C gave 57% conversion of aldehyde, TON of 236 and TOF of 8.7 $h^{-1}$ (27 hours of reaction). However the reaction with heptaldehyde was not selective as heptanoic acid was also formed as by-product.

The other compounds were also tested in the Knöevenagel condensation of benzaldehyde with malononitrile in 4.0 mL of

toluene at 60°C at the same time using a Radleys Carousel. The kinetic profile of the reactions is presented in Fig. S8. It can be seen for **1** that the reaction progressed slower than in 1.0 mL of toluene and in a smaller reactor. Nevertheless, the most active are **1** and **2**, whereas **3** and **4** show similar catalytic activity. This also shows that the presence of lanthanides is important for the course of the reaction.

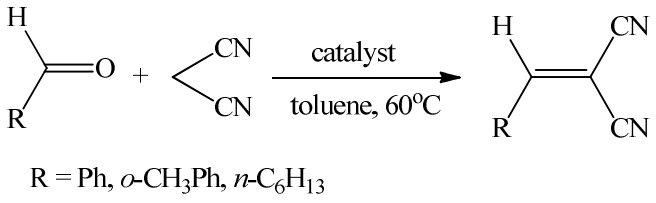


R = Ph, *o*-$CH_3$Ph, *n*-$C_6H_{13}$

Fig. 8 Knöevenagel condensation of benzaldehyde with malononitrile.

The MOFs only contain Lewis acid sites and Knöevenagel condensation has been reported to traditionally being catalysed by base catalysts.[53] However, copper(II) benzene-1,3,5-tricarboxylate (CuBTC) metal-organic framework was found be an effective heterogeneous catalyst for the Knöevenagel condensation despite containing Lewis acid sites.[53] A mechanism was proposed where the CuBTC works as a Bronsted base in the reaction and deprotonates the active methylene group of malononitrile. A Bronsted acid defect site is thus formed in the MOF and together with the adjacent Lewis acid (iron and rare earth ions) facilitate the activation of both reactants in the Knöevenagel condensation.[53] The deprotonated active methylene group of malononitrile attacks the aldehyde and then after re-protonation and dehydration of the adduct the Knöevenagel condensation product is formed.[53]

## Conclusions

In summary, four new 3*d*-4*f* hetero-metal organic phosphonate frameworks, $[LnFe^{III}Fe^{II}_6(Hpmida)_6]\cdot 2H_2O$ {Ln = Eu (**1**), Dy (**2**), Ho (**3**) and Y (**4**), pmida: *N*-(phosphonomethyl)iminodiacetic acid} were synthesized via ionothermal methodology. The coordination polymers feature a very interesting 3-D framework built up from a secondary building unit, $[Fe_2(Hpmida)_2]^{2-}$, further connecting six coordinated $Eu^{3+}$ and $Fe^{3+}$ cations and possess a new topology type with the point symbol of $\{4^{12}\cdot 6^3\}_2\{4^3\}_6\{4^6\cdot 8^6\cdot 10^3\}\{4^8\cdot 6^6\cdot 8\}_6$ and complicated unique tilings. The catalytic property of **1**–**4** indicates that this type of compounds are a truly heterogeneous catalyst in the Knöevenagel condensation with high selectivity.

## Acknowledgements

We thank Fundação para a Ciência e a Tecnologia (FCT), FEDER, QREN, COMPETE (PEst-C/CTM/LA0011/2013) and (FCT: SFRH/BPD/74582/2010) for financial support. F.-N. SHI acknowledges FCT for the project of PTDC/CTM-NAN/119994/2010. T.-H. Yang acknowledges the NSF of Jiangsu Province (BK20140244), The Project Sponsored by the Scientific Research Foundation for Returned Overseas Chinese Scholars of State Education Ministry, the NSF for Universities in Jiangsu Province (13KJB150013), the Science and Technology Bureau of Changzhou City (No. CJ20140031) and Jiangsu University of Technology (KYY13035).

## Notes and references

[a] School of Chemistry & Environmental Engineering, Jiangsu University of Technology, Changzhou 23001, P R China. Fax: +86-519-86953269; Tel: +86-519-86953269; E-mail: tinghai_yang@hotmail.com, fshi96@foxmail.com.

[b] School of Science, Shenyang University of Technology, 110870, Shenyang, P R China.

[c] Department of Chemistry, CICECO, University of Aveiro, 3810-193 Aveiro, Portugal.

[d] Department of Physics, CICECO, University of Aveiro, 3810-193 Aveiro, Portugal.

† Electronic Supplementary Information (ESI) available: IR data，TG catalytic data and table of elected bond lengths and angle of **1**−**4**. CCDC 1055583-1055586. For ESI and crystallographic data in CIF or other format see DOI: 10.1039/b000000x/

1 P. Wasserscheid and T. Welton, *Ionic Liquids in Synthesis*, Wiley-VCH: Weinheim, Germany, 2003.
2 E. R. Cooper, C. D. Andrews, P. S. Wheatley, P. B. Webb, P. Wormald and R. E. Morris, *Nature*, 2004, **430**, 1012-1016.
3 D. Freudenmann, S. Wolf, M. Wolff and C. Feldmann, *Angew. Chem., Int. Ed.*, 2011, **50**, 11050-11060.
4 N. V. Plechkova and K. R. Seddon, *Chem. Soc. Rev.*, 2008, **37**, 123-150.
5 E. R. Parnham and R. E. Morris, *Accounts. Chem. Res.*, 2007, **40**, 1005-1013.
6 V. I. Pârvulescu and C. Hardacre, *Chem. Rev.*, 2007, **107**, 2615-2665.
7 H. Fu, C. Qin, Y. Lu, Z.-M. Zhang, Y.-G. Li, Z.-M. Su, W.-L. Li and E.-B. Wang, *Angew. Chem., Int. Ed.*, 2012, **51**, 7985-7989.
8 J. Zhang, S. Chen and X. Bu, *Angew. Chem., Int. Ed.*, 2008, **47**, 5434-5437.
9 Z. Lin, A. M. Z. Slawin and R. E. Morris, *J. Am. Chem. Soc.*, 2007, **129**, 4880-4881.
10 T. G. Parker, J. N. Cross, M. J. Polinski, J. Lin and T. E. Albrecht-Schmitt, *Cryst. Growth Des.*, 2014, **14**, 228-235.
11 Y. Meng, J.-L. Liu, Z.-M. Zhang, W.-Q. Lin, Z.-J. Lin and M.-L. Tong, *Dalton Trans.*, 2013, **42**, 12853.
12 Q.-Y. Liu, W.-L. Xiong, C.-M. Liu, Y.-L. Wang, J.-J. Wei, Z.-J. Xiahou and L.-H. Xiong, *Inorg. Chem.*, 2013, **52**, 6773-6775.
13 S. Li, W. Wang, L. Liu and J. Dong, *Crystengcomm*, 2013, **15**, 6424.
14 J. Chen, S.-H. Wang, Z.-F. Liu, M.-F. Wu, Y. Xiao, F.-K. Zheng, G.-C. Guo and J.-S. Huang, *New J. Chem.*, 2014, **38**, 269-276.
15 B. An, Y. Bai, J.-L. Wang and D.-B. Dang, *Dalton Trans.*, 2014, **43**, 12828.
16 Z. Lin, D. S. Wragg, J. E. Warren and R. E. Morris, *J. Am. Chem. Soc.*, 2007, **129**, 10334-10335.
17 K. Li , Z. Tian, X. Li, R. Xu, Y. Xu, L. Wang, H. Ma, B. Wang and L. Lin, *Angew. Chem., Int. Ed.*, 2012, **51**, 4397-4400.
18 W.-J. Ji, Q.-G. Zhai, S.-N. Li, Y.-C. Jiang and M.-C. Hu, *Chem. Commun.*, 2011, **47**, 3834-3836.

 

19 L. Xu, Y.-U. Kwon, B. de Castro and L. Cunha-Silva, *Cryst. Growth Des.*, 2013, **13**, 1260-1266.
20 Q.-Y. Liu, Y.-L. Li, Y.-L. Wang, C.-M. Liu, L.-W. Ding and Y. Liu, *CrystEngComm*, 2014, **16**, 486-491.
21 J. Rocha, F. A. Almeida Paz, F.-N. Shi, D. Ananias, N. J. O. Silva, L. D. Carlos and T. Trindade, *Eur. J. Inorg. Chem.*, 2011, **2011**, 2035-2044.
22 F.-N. Shi, T. Trindade, J. Rocha and F. A. A. Paz, *Cryst. Growth Des.*, 2008, **8**, 3917-3920.
23 M. Sakamoto, K. Manseki and H. Okawa, *Coord. Chem. Rev.*, 2001, **219**, 379-414.
24 C. Benelli and D. Gatteschi, *Chem. Rev.*, 2002, **102**, 2369-2387.
25 C. E. Plecnik, S. M. Liu and S. G. Shore, *Acc. Chem. Res.*, 2003, **36**, 499-508.
26 J.-L. Liu, Y.-C. Chen, F.-S. Guo and M.-L. Tong, *Coordin. Chem. Rev.*, 2014, **281**, 26-49.
27 G. Peng, L. Ma, L. Liang, Y. Z. Ma, C. F. Yang and H. Deng, *CrystEngComm*, 2013, **15**, 922-930.
28 J. B. Peng, Q. C. Zhang, X. J. Kong, Y. Z. Zheng, Y. P. Ren, L. S. Long, R. B. Huang, L. S. Zheng and Z. P. Zheng, *J. Am. Chem. Soc.*, 2012, **134**, 3314-3317.
29 T.-H. Yang, A. R. Silva and F.-N. Shi, *Dalton Trans.*, 2013, **42**, 13997.
30 C.-J. Shen, S.-M. Hu, T.-L. Sheng, Z.-Z. Xue and X.-T. Wu, *Dalton Trans.*, 2015.
31 F. Luo, Y.-T Yang, Y.-X. Che and J.-M. Zheng, *CrystEngComm*, 2008, **10**, 1613-1616.
32 Y. Zhou, M. Hong and X. Wu, *Chem. Commun.*, 2006, 135-143.
33 G.-L. Zhuang, W.-X. Chen, G.-N. Zeng, J.-G. Wang and W.-l. Chen, *CrystEngComm*, 2012, **14**, 679-683.
34 G.-L. Zhuang, X.-J. Sun, L.-S. Long, R.-B. Huang and L.-S. Zheng, *Dalton Trans.*, 2009, 4640-4642.
35 X.-J. Kong, L.-S. Long, R.-B. Huang, L.-S. Zheng, T. D. Harris and Z. Zheng, *Chem. Commun.*, 2009, 4354-4356.
36 X. Feng, Y.-Q. Feng, J. J. Chen, S.-W. Ng, L.-Y. Wang and J.-Z. Guo, *Dalton Trans.*, 2015, **44**, 804-816.
37 S.-L. Cai, S.-R. Zheng, Z.-Z. Wen, J. Fan and W.-G. Zhang, *CrystEngComm*, 2012, **14**, 8236-8243.
38 Y.-Q. Sun, J. Zhang and G.-Y. Yang, *Chem. Commun.*, 2006, 4700-4702.
39 G. Peng, Z. H. Liu, L. Ma, L. Liang, L. M. Zhang, G. E. Kostakis and H. Deng, *CrystEngComm*, 2012, **14**, 5974-5984.
40 C.-J. Li, Z.-J. Lin, M.-X. Peng, J.-D. Leng, M.-M. Yang and M.-L. Tong, *Chem. Commun.*, 2008, 6348-6350.
41 H.-M. Peng, H.-G. Jin, Z.-G. Gu, X.-J. Hong, M.-F. Wang, H.-Y. Jia, S.-H. Xu and Y.-P. Cai, *Eur. J. Inorg. Chem.*, 2012, **2012**, 5562-5570.
42 Z.-G. Gu and S. C. Sevov, *J. Mater. Chem.*, 2009, **19**, 8442.
43 Y.-H. Su, S. S. Bao and L.-M. Zheng, *Inorg. Chem.*, 2014, **53**, 6042-6047.
44 Y.-S. Ma, H. Li, J.-J. Wang, S.-S. Bao, R. Cao, Y.-Z. Li, J. Ma and L.-M. Zheng, *Chem. – Eur. J.*, 2007, **13**, 4759-4769.
45 *SAINT+, Data Integration Engine, v. 7.23a*, Bruker AXS, Madison, Wisconsin, 1997-2005.
46 G. M. Sheldrick, *SHELXS-97, Program for Crystal Structure Solution*, University of Göttingen, Germany, 1997.
47 G. M. Sheldrick, *SHELXL-97, Program for Crystal Structure Refinement*, University of Göttingen, Germany, 1997.
48 S.-L. Cai, S.-R. Zheng, Z.-Z. Wen, J. Fan, N. Wang and W.-G. Zhang, *Cryst. Growth Des.*, 2012, **12**, 4441-4449.
49 A. Baniodeh, I. J. Hewitt, V. Mereacre, Y. Lan, G. Novitchi, C. E. Anson and A. K. Powell, *Dalton Transactions*, 2011, **40**, 4080-4086.
50 V. A. Blatov and A. P. Shevchenko, *TOPOS–Version Professional beta evaluation*, Samara State University, Samara, Russia, 2006.
51 M. Opanasenko, A. Dhakshinamoorthy, J. Čejka and H. Garcia, *ChemCatChem*, 2013, **5**, 1553-1561.
52 Y. Yang, H.-F. Yao, F.-G. Xi and E.-Q. Gao, *J. Mol. Catal. A: Chem.*, 2014, **390**, 198-205.
53 M. Polozij, M. Rubes, J. Cejka, P. Nachtigall, *ChemCatChem* , 2014, **6**, 2821-2824.